Positron Acceleration by Plasma Wakefields Driven by a Hollow Electron Beam

Neeraj Jain, T. M. Antonsen, Jr., and J. P. Palastro

Phys. Rev. Lett. **115**, 195001 — Published 5 November 2015

DOI: 10.1103/PhysRevLett.115.195001

Positron acceleration by plasma wakefields driven by a hollow electron beam

Neeraj Jain*

Max Planck Institute for Solar System Research,

Justus-von-Liebig-Weg 3, 37077, Göttingen, Germany

T. M. Antonsen Jr.

Institute for Research in electronics and Applied Physics,

University of Maryland, College Park, MD, USA

J. P. Palastro*

Naval Research Laboratory, Washington DC 20375-5346, USA

(Dated: October 7, 2015)

Abstract

A scheme for positron plasma wakefield acceleration using hollow or donut shaped electron driver beams is studied. An annular shaped, electron free region forms around the hollow driver beam creating a favorable region (longitudinal field is accelerating and transverse field is focusing) for positron acceleration. For FACET like parameters, the hollow beam driver produces accelerating gradients on the order of 10 GV/m. The accelerating gradient increases linearly with the total charge in the driver beam. Simulations show acceleration of a 23 GeV positron beam to 35.4 GeV with a maximum energy spread of 0.4% and very small emittance over a plasma length of 140 cm is possible.

The plasma based particle acceleration schemes, first proposed in 1979 [1], have already achieved acceleration gradients ($\sim$ tens of GeV/m) much larger than those ($\sim$ tens of MeV/m) in conventional radio frequency accelerators. In plasma based particle acceleration schemes, a high intensity laser or an ultra-relativistic charged particle beam propagates through a plasma generating electromagnetic fields in its wake. In the so called bubble regime of Plasma Wakefield Acceleration (PWFA) [2–4], all the plasma electrons are expelled from the path behind a short (approximately one plasma wavelength $k_p^{-1} = c/\omega_p$ long) and dense (beam density > plasma density) electron beam driver forming an electron free region known as a bubble or ion channel. The expelled electrons then fall back to the beam propagation axis behind the driver. The blowout regime offers a nearly radially uniform high acceleration gradient for efficient acceleration of electrons. The electron acceleration to high energies (energy doubling of 43 GeV electrons in an 85 cm long plasma) has been demonstrated in PWFA experiments [5]. Plasma-based acceleration of positrons, on the other hand, has been less explored and is essential for a successful operation of a wakefield-based electron-positron collider.

Current positron acceleration schemes generate wakefields in plasma either by an electron [6] or by a positron beam driver [7]. When the wakefields are driven by an electron beam driver in the bubble regime, the favorable region for positron acceleration (transverse field focusing and longitudinal field accelerating) forms between the first and second bubble. The favorable region has a narrow extent between the two bubbles. The accelerating electric field varies rapidly with axial coordinate leading to large energy spread in the accelerated positron beam (witness beam). Furthermore, the transverse focusing field causes an increase in the emittance of the witness beam. In the case of a positron driver, the plasma electrons are attracted towards, rather than blown out of, the driver beam path and do not cross the axis in a narrow region as they do in case of electron beam driver [7]. As a result the accelerating fields are smaller than those driven by electron beams. The focusing fields are nonlinear in the transverse coordinate and vary along the axis of the beam leading to the emittance growth of the witness beam. The accelerating gradients can be improved if the positron beam driver propagates through a hollow plasma channel [7]. For an appropriate hollow plasma channel radius, plasma electrons can cross the axis in a narrow region increasing the wakefield amplitude.

In this Letter, we present a scheme of wakefield generation for positron acceleration

using hollow or donut shaped electron drive beams (the beam density is maximum at an off axis location). Recently, self injection of hollow electron bunch in the wakefields driven by a Laguerre-Gaussian laser pulse and positron acceleration was observed in simulations [8]. The hollow electron beam pushes the plasma electrons towards its axis setting up the wakefields for positron acceleration in the hollow region. The accelerating field for positrons increases with the total charge in the beam driver while the axial size of the favorable region ($\sim$ one plasma wavelength) remains approximately unchanged. This is in contrast to the case of solid beam driver in which the size of the favorable region diminishes with increasing charge in the beam [6].

We calculate wakefields driven by the propagation of a hollow electron beam in a uniform plasma in an azimuthally symmetric ($\partial/\partial\theta = 0$) cylindrical geometry using the quasi-static code WAKE [9]. The quasi-static approximation exploits the disparity of driver and plasma evolution time scales. The time scale of evolution of the ultra-relativistic electron beam (relativistic factor $\gamma_b >> 1$) is the betatron period $\tau_b = \sqrt{2\gamma_b}\lambda_p/c$ which is much larger than the plasma time scale λ_p/c, where λ_p is the plasma wavelength. In the code WAKE, the response of the kinetic, warm and relativistic plasma is calculated on a fast time scale assuming a fixed beam driver. The driver is then evolved over longer time scales [10].

We employ a moving computational domain which changes its axial position as the beam driver propagates along the axis. The axial coordinate (ξ) in the moving computational domain can be written as $\xi = ct - z$. The initial number density of the hollow or donut shaped electron beam driver is expressed as,

$$n_{beam} = n_b \exp\left[-\frac{(r-r_0)^2}{2\sigma_r^2} - \frac{(\xi-\xi_0)^2}{2\sigma_z^2}\right] \tag{1}$$

The peak number density (n_b) of the hollow beam is located at an off axis location (r_0, ξ_0) and falls off within distances σ_r (radially) and σ_z (axially). The beam is completely hollow in the limit $r_0/\sigma_r \to \infty$. Otherwise there is a small but finite density in the core of the beam. In the limit $r_0 \to 0$, the beam density has its peak at the axis and corresponds to a solid beam.

We first study wakefield generation by a non-evolving electron driver (Driver evolution will be addressed subsequently). In the simulations, plasma density is uniform. The beam is axially centered at $\xi_0 = 0$ and $k_p\sigma_z = 2$ for all the results presented here for non-evolving driver. We vary the values of σ_r, r_0 and the total charge $Q_d = -e\int n_{beam}(r,\xi) r\, dr\, d\theta\, d\xi$

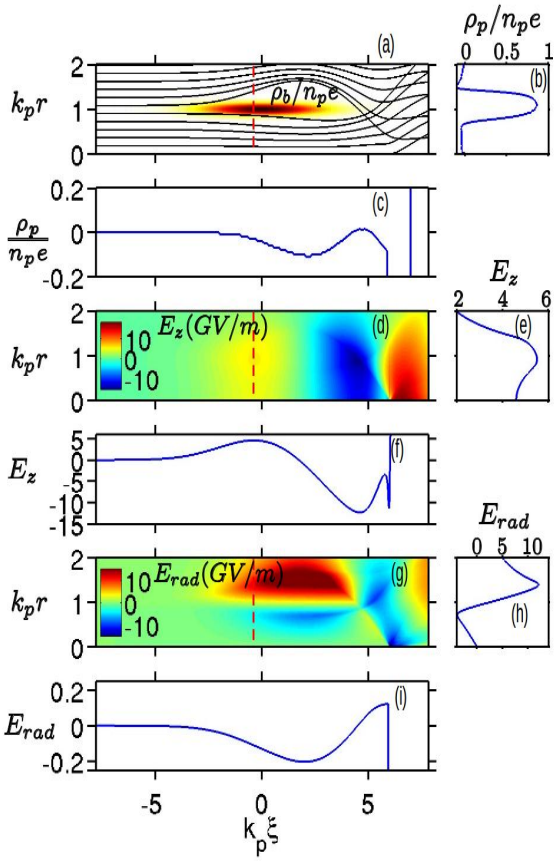

FIG. 1. Trajectories of plasma electrons and driver beam density ρ_b (a), longitudinal electric field E_z (d) and transverse field $E_{rad} = E_r - cB_\theta$ (g) in the $r-\xi$ simulation domain for a hollow electron beam driver ($k_p\sigma_r = 0.1$, $k_pr_0 = 1$ and $Q_d = 0.8$ nC). On axis longitudinal line-outs of plasma charge density ρ_p (c), E_z (f) and E_{rad} (i). Transverse line-outs along the vertical red-dashed line (at ξ-location of maximum E_z) of ρ_p (b), E_z (e) and E_{rad}(h). The color scale for E_{rad} is saturated at -15 GV/m in order to improve the visibility of the negative (focusing for positrons) transverse field in the region $k_pr < 1$.

contained in the driver. The beam driver with an initial energy 23 GeV is modeled using 4×10^6 simulation particles. The plasma is modeled using 9 particles per cell. The simulation domain sizes along r and ξ are $10\,k_p^{-1}$ and $15.6\,k_p^{-1}$ with a grid resolutions of $0.02\,k_p^{-1}$ and $0.03\,k_p^{-1}$, respectively. The wakefields, shown in Figs. 1-3, are in the units of GV/m calculated for the plasma density $n_p = 2 \times 10^{17}$ cm^{-3} (typical plasma density in FACET [11]) giving $k_p^{-1} = c/\omega_{pe} = 12\,\mu$m.

In response to a hollow electron beam driver, plasma electrons are expelled from the

region of the beam and their trajectories are shown in Fig. 1a. Since the bulk of the hollow beam is centered off axis, the plasma electrons are expelled both towards and away from the axis. This is in contrast with the case of a solid beam in which plasma electrons are expelled only away from the axis. The plasma electrons move towards the axis through the hollow region and experience a repulsive force due to other plasma electrons converging towards the axis. For this reason, the radial deflection of plasma electron trajectories in the hollow region is small until they intersect the back of the bubble. At the back of the driver, plasma electrons are pulled back (towards their original radial position) by the annular shaped electron free region.

The resulting structures of the wakefields are shown in Figs. 1d and 1g. The longitudinal electric field E_z for the hollow beam driver is structurally the same as for the solid beam driver. However, the structure of the transverse field $E_{rad} = E_r - cB_\theta$ is different. The transverse field in the hollow region of the beam ($r < r_0$) is radially inward, and thus, focusing for positrons. The reason for the radially inward transverse field is the formation of an annular shaped electron free region which has positive charge density due to background ions. Since the net charge density of plasma $\rho_p = e(n_p - n_e)$ below and above the electron free region is negative due to excess plasma electrons (see Fig. 1a and b), the transverse wakefield points radially inward and outward near the bottom and top boundaries of the electron free region, respectively.

The longitudinal electric field is positive in a part of the region where the transverse force is focusing for positrons. The axial line-outs of E_z along the axis ($r = 0$) and of E_{rad} just above the axis, Figs. 1f and 1i, show that the axial size of the favorable region for positron acceleration (positive E_z and negative $E_r - cB_\theta$) is of the order of a plasma wavelength $\lambda_p = 2\pi/k_p$. For efficient acceleration of a positron bunch, E_z needs to be radially and axially uniform for minimizing the energy spread, and E_{rad} needs to be axially uniform but varying linearly in the radial direction for emittance preservation. The magnitudes of E_z and E_{rad} in the favorable region vary with ξ, however, the variations are not as rapid as they are in the favorable region for positron acceleration behind the first bubble formed by a solid beam driver. Although the transverse field in the favorable region is focusing for positrons until $r \approx r_0$, its radial variation can be approximated as linear only before it reaches its negative peak as can be seen in radial line-out of E_{rad} in Fig. 1h. We define approximately the radial size Δ_R of the favorable region for positron acceleration as the radial distance

at which $dE_{rad}/dr = 0$. This definition considers only the linear radial-dependence of the focusing field and thus provides a conservative estimate of the radial size of the favorable region for positron acceleration. With nonlinear focusing forces, positrons can be focused over a wider region (up to $r \approx r_0$, see Fig. 1h). The radial line-out of E_z in Fig. 1e shows that, close to the axis, E_z is quite uniform in the radial direction The radial uniformity and relatively slow variation with ξ of E_z are ideal for positron acceleration with low energy spread.

Fig. 2(a-f) shows the variations of E_z^{max} (maximum on-axis longitudinal electric field) and Δ_R with the hollow beam parameters, r_0 and σ_r, for a fixed amount of total charge $Q_d = 0.8$ nC contained in the hollow beam driver. The maximum on-axis electric field E_z^{max} drops rapidly with r_0 but is only weakly dependent on σ_r (specially when $r_0/\sigma_r >> 1$). On increasing r_0, the influence of the driver beam charge on the plasma electrons near the axis becomes weaker reducing the plasma density perturbation and hence the on-axis electric field. In the limit $r_0/\sigma_r \to \infty$ plasma electrons near the axis see the beam driver as a ring of charge, and thus the weak dependence of E_z^{max} on σ_r.

Since the plasma density perturbation close to the axis is much smaller than the background plasma density, the dependence of E_z^{max} on r_0, σ_r can be well approximated by linear theory[12] according to which the on-axis longitudinal electric field for the hollow beam driver, assuming $r_0/\sigma_r >> 1$, is given by,

$$E_z(0,\xi) = \sqrt{\frac{2}{\pi}} \left[\frac{Q_d R(0)}{\sigma_r r_0}\right] e^{-k_p^2\sigma_z^2/2} \cos(k_p\xi), \tag{2}$$

$$R(0) = k_p^2 \int_0^\infty r' dr' e^{-(r'-r_0)^2/2\sigma_r^2} K_0(k_p r'). \tag{3}$$

Here K_0 is the modified Bessel function of zero-order. The amplitude of $E_z(0,\xi)$ calculated using Eq. (2) compares well (within much less than an order of magnitude) with E_z^{max} obtained from simulations, as shown in Figs. 2b and 2c.

The radial size Δ_R is non-zero only above a critical value of $r_0/\sigma_r \approx 3$. This is because the driver beam density, which has a radial Gaussian profile (Eq. 1), is negligibly small on the beam axis for $r_0/\sigma_r > 3$, and the plasma electrons respond to the hollow driver as shown in Fig. 1a. However when $r_0/\sigma_r < 3$, the beam density on the axis is finite and may cause the plasma electrons near the axis to respond similarly to the case of solid beam driver generating a radial wakefield which de-focuses the positrons in the neighborhood of the axis. For $r_0/\sigma_r > 3$, Δ_R decreases (increases) with σ_r (r_0) , (see Figs. 2(d-f)). On increasing

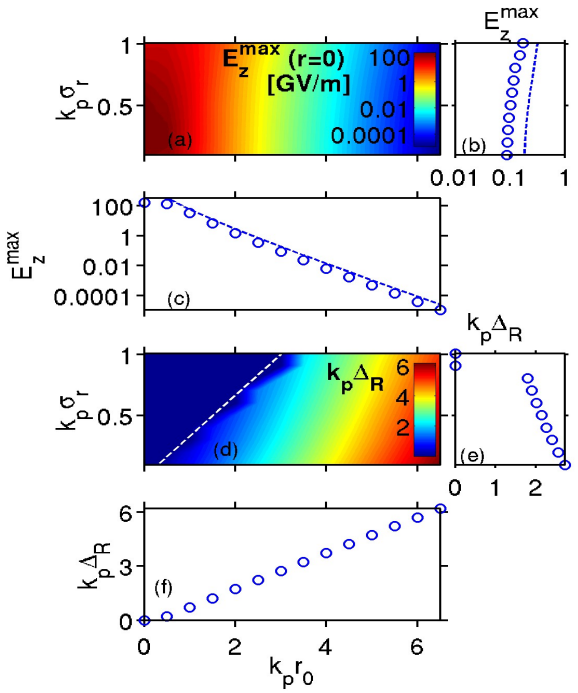

FIG. 2. Color plots: maximum on-axis longitudinal electric field $E_z^{max}(r=0)$ in log-scale (a) and radial size Δ_R of the favorable region (d) as functions of r_0 and σ_r for a hollow electron beam driver with total charge $Q_d = 0.8$ nC. On the white-dashed line in (d), $r_0/\sigma_r = 3$. Lineouts of E_z^{max} (c) and Δ_R (f) along r_0-axis for $k_p\sigma_r = 0.1$. Lineouts of E_z^{max} (b) and Δ_R (e) along σ_r-axis for $k_p r_0 = 3$. The dashed lines in (b) and (c) are E_z^{max} calculated from the linear theory.

r_0 or decreasing σ_r, the bulk of the driver beam shifts away from the axis allowing a larger radial extent of excess electron density in the hollow region and thus a larger radial size Δ_R of the favorable region.

A scaling relation for Δ_R can be obtained by approximating the structure of the perturbed plasma density by step-functions ($n_{wake} = n_\Delta$ for $r < \Delta_R$ and $n_{wake} = n_p$ for $\Delta_R < r < R$, where $r_0 < R < R_b$ and R_b is the radius of the upper plasma electron sheath) in the radial direction and uniform along ξ. Although this representation of the plasma density is not correct near $r = R_b$, it is good enough for our purpose of calculating fields only up to $r \approx r_0 + 5\sigma_r$ (in a distance of $5\sigma_r$, beam density almost vanishes). Conservation of number of electrons, $n_p r_0^2 = n_e \Delta_R^2$ where $n_e = n_p + n_\Delta$ gives,

$$\Delta_R \approx (1 - n_\Delta/2n_p) r_0 \tag{4}$$

for $n_\Delta << n_p$. For large r_0/σ_r, n_Δ should depend only on σ_r. The linear scaling of Δ_R with

r_0 with a slope slightly smaller than unity, Eq. (4), agrees well with the simulation results shown in Fig. 2f. The dependence of Δ_R on σ_r should come through n_Δ.

On increasing Q_d, the total charge in the hollow beam driver, the plasma electrons are pushed harder towards the axis, thus increasing the plasma density perturbation near the axis and decreasing the radial size Δ_R. Although the radial extent Δ_R decreases with Q_d, it remains of the order of k_p^{-1} for up to Q_d=8 nC (Fig. 3a). Fig 3b shows that E_z^{max} increases linearly with the total charge Q_d. The linear scaling of E_z^{max} with Q_d is evident from the linear theory, Eq. (2), and is in good agreement with the one obtained from the simulations, as shown in Fig. 3b.

The axial size of the favorable region for positron acceleration (not shown) increases only by a small length. This is unlike the favorable region for positron acceleration in the back of the solid beam driver. In the latter case, the axial size of the favorable region shrinks with the energy content of the driven plasma wave and thus increasing the charge in the beam does not improve the efficiency. The focusing field driven by the hollow beam driver varies faster with ξ for larger values of Q_d (not shown). However, this variation of the focusing field is still slower than that in the back of the solid beam driver.

Now, we show by simulations that a witness beam of positrons can be efficiently accelerated in the wakefields generated by a hollow, evolving, electron beam driver. For this purpose we place a positron beam with a density profile given by,

$$n_{witness} = n_w \exp\left[-\frac{r^2}{2\sigma_{r,w}^2} - \frac{(\xi-\xi_w)^2}{2\sigma_{z,w}^2}\right], \tag{5}$$

on the axis of an evolving hollow electron beam driver whose initial density profile is given by Eq. (1). The background plasma has a uniform density, $n_p = 5\times10^{16}$ cm^{-3} giving $k_p^{-1} = 23.79\,\mu$m, and is modeled using 9 simulation particles per cell. The parameters for electron beam driver are $\xi_0 = 0$, $k_p\sigma_z = 1$, $k_p\sigma_r = 0.2$, $k_p r_0 = 2$ and $n_b/n_p = 3$ (total charge $Q_d = -5.12$ nC). The initial emittance of the electron driver is zero. The witness bunch parameters are $k_p\sigma_{z,w} = k_p\sigma_{r,w} = 0.2$, $k_p\xi_w = 0.26$ and $n_b/n_p = 1$ (total charge in witness bunch $Q_w = 13.58$ pC). The electrons in the driver and positrons in the witness beam have an initial energy of 23 GeV and are modeled using 1.25 $\times10^6$ and 6.25 $\times10^5$ simulation particles, respectively. The simulation domain size along ξ is approximately $11\,k_p^{-1}$ with a grid resolution $k_p d\xi = 0.02$ while along r is $\approx 5\,k_p^{-1}$ with a grid resolution of $k_p dr \approx 0.025$. The driver and witness beams are propagated in the uniform plasma in steps of $ds \approx 4.75\,\mu$m

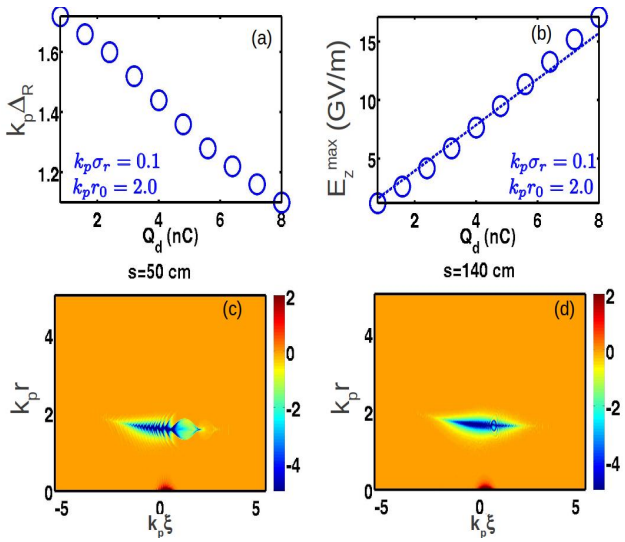

FIG. 3. Scaling of Δ_R (a) and $E_z^{max}(r=0)$ (b) with the total charge Q_d in the hollow beam driver ($k_p\sigma_r = 0.1$, $k_pr_0 = 2.0$) obtained from simulations (open circles) and linear theory (dashed line). Charge densities of the driver (electrons) and witness (positrons) beams after they have propagated a distance $s = 50$ cm (c) and $s = 140$ cm (d). The color scale for charge density is saturated at -5.0 and 2.0.

for a total distance of 140 cm.

Figures 3c and 3d show charge densities of the driver and witness beams after propagating 50 and 140 cm. Fish-bone like structures in the electron beam driver, which initially had Gaussian shape (Fig. 1a), can be seen at $s = 50$ cm. These structures develop because the slope $[dE_{rad}/dr]_{E_{rad}=0}$ of $E_{rad} \propto r$ (near the peak density of the driver beam) varies with ξ (see Fig. 1g and 1h), resulting in the ξ-variation of the betatron time period $\tau_\beta = 2\pi\sqrt{\gamma_b/[dE_{rad}/dr]_{E_{rad}=0}}$, where γ_b is the relativistic factor of the driver beam particles. As a consequence the beam particles, at a given propagation distance s, are in different phases of the oscillations. Later (s=140 cm) the oscillations have phase mixed because the phase difference between the oscillations at two ξ-locations is not constant in time.

The evolution of electron beam driver does not affect the wakefield structure for positron acceleration. In fact, the radial extent of the electron beam driver shrinks during the propagation, thereby reducing the effective value of σ_r. As a result, the longitudinal electric field E_z also increases in and around the axial extent of the witness beam. However, as shown in Fig. 4a, E_z saturates at slightly larger values by $s \approx 50$ cm. The energy gain of the witness

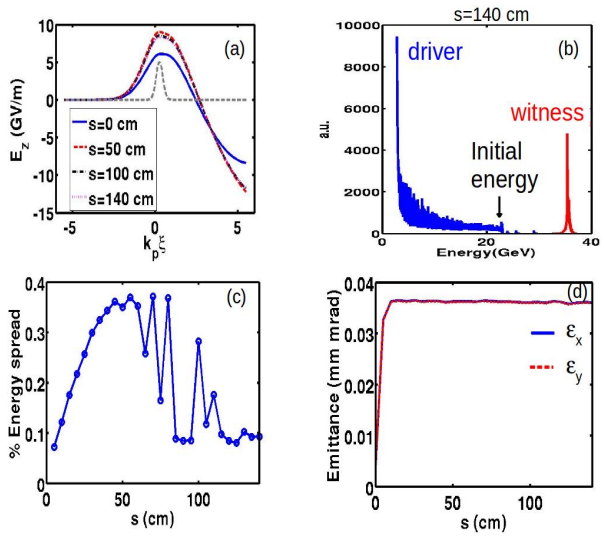

FIG. 4. Line-outs of longitudinal electric field E_z (at various propagation distances) and initial profile of witness (positrons) charge density (gray dashed line; in arbitrary units) along the axis ($r = 0$) (a). Energy spectrum of driver and witness beams after 140 cm of propagation in plasma (b). Energy spread in percentage (c) and normalized RMS x and y emittance (d) in witness beam as a function of propagation distance s.

beam after propagating 140 cm is 12.4 GeV in Fig. 4b. The estimate of work done by the electric field can be obtained from $W = e\int_0^{140\text{cm}} E_z^{peak}(s)ds \approx 12.43$ GeV, where E_z^{peak} is the maximum value of E_z on the axis. This estimate is very close to the energy gained by the witness beam.

The axial position of the witness beam was chosen to produce and sit in a uniform region of E_z. This uniform region becomes slightly nonuniform due to beam evolution. However it does not significantly affect the energy spread of the accelerated witness beam as can be seen in Fig. 4c. The percentage energy spread of the witness beam defined as $(\Delta K_{fwhm}/K_{max}) \times 100$ first increases and then decreases with the propagation distance. Here ΔK_{fwhm} is the full width at half maximum of the energy spectrum of the witness beam and K_{max} is the energy corresponding to the peak of the energy spectrum, Fig. 4b. The maximum value of the percentage energy spread remains under 0.4. In Fig. 4d, the normalized RMS emittance of the witness beam, ϵ_x and ϵ_y (defined as $\epsilon_x = \sqrt{< x^2 >< p_x^2 > - < xp_x >^2}/m_e c$ where x and p_x are the position and momentum of a witness particle, and similar definition for ϵ_y), does not increase much and remains close to its initial value during the beam's propagation.

The most attractive feature of this scheme is the linear scaling of the longitudinal electric field with the charge in the driver beam without compromising the size of the favorable region. For appropriate beam (Q_d, r_0 and σ_r) and plasma (n_0) parameters, a hollow electron beam driver can produce radially uniform accelerating gradient in excess of 10 GV/m and sufficiently large favorable region for positron acceleration. For example, $E_z^{max} \approx$17 GV/m, radial size $\Delta_R \approx k_p^{-1} \approx 12\,\mu$m and axial size $\lambda_p \approx 2\pi/k_p \approx 75\,\mu$m for the hollow beam parameters, $Q_d = 8$ nC, $k_p r_0 = 2.0$ and $k_p\sigma_r = 0.1$, and plasma density $n_0 = 2 \times 10^{17}$ cm^{-3} (Fig. 2g and 2h). These radial and axial sizes are large enough for the placement of a positron beam of available size (radial size ≈ 10 μm and axial size $< 100\,\mu$m[11]). Even radially wider positron beams with $\Delta_R < \sigma_{r,w} < r_0$ can also be focused albeit with nonlinear focusing forces.

Recent simulations reported that very high accelerating and focusing wakefields ~ 1000 GV/m for positrons can be driven by a Laguerre-Gaussian laser pulse [8]. The energy gain of the positron beam will be limited by radiation losses due to the betatron oscillations of positrons in such a high focusing wakefield. For net energy gain, the radiated power $P = 2r_e^2 c\gamma^2 E_{rad}^2/3$ ($r_e = e^2/m_e c^2$ is classical electron radius and γ is the relativistic factor of positrons) [13] must be less than the gained power $G = eE_z c$ ($E_z \sim E_{rad}$). The condition $P < G$ restricts the energy of the positrons $K[\mathrm{GeV}] = \gamma m_e c^2 < (75000/E_{rad}[\mathrm{GV/m}])^{1/2}$ below $K < 8.66$ GeV for E_{rad} =1000 GV/m. Reducing the focusing field by tuning laser and plasma parameters will also reduce the accelerating field and then the laser pulse needs to propagate in plasma for longer distances for same energy gain. In general, laser propagation in a plasma for long distances (of the order of few meters) is limited by their nonlinear evolution. On the other hand, hollow electron beam drives moderate accelerating and focusing wakefields for positrons, thus reducing the radiative losses. At the same time, it is self guided and its evolution does not affect the wakefield structure for positron acceleration for propagation distances of the order of a meter.

In conclusion, we demonstrated by 2-D kinetic simulations an efficient scheme of positron acceleration to high energies in a meter scale plasma. However, one may suspect that, in 3-D, the hollow beam driver might be subjected to azimuthal Weibel instability. The instability appears when the plasma provides a return current such that the net current is zero [14]. The counter directed plasma and beam currents repel causing the currents to filament. The instability is suppressed by transverse temperature. A thorough study of the instability

for the case of a hollow beam driver would need to include both a 3D description of the fields and inclusion of driver beam emmittance. This is beyond the scope of the present investigation.

We observe that the hollow electron beam breaks up after propagating a certain distance in the plasma, e.g., after 160 cm for the case shown in Fig. 3. The evolution of the beam driver depends on the beam (r_0, σ_r, Q_d and emittance) and plasma parameters (n_0). The break up of the beam can be avoided/delayed by matching the beam parameters to the plasma parameters such that the hollow beam driver propagates in the plasma with a constant radius. The 3-D evolution and matched propagation of the hollow electron beam driver are the subjects of our future studies.

This work was supported by the US DoE grant number DESC0007970.

---

* Work done at Institute for Research in Electronics and Applied Physics, University of Maryland, College Park, MD, USA and supported by the US DoE.

[1] T. Tajima and J. M. Dawson, Phys. Rev. Lett. **43**, 267 (1979).

[2] P. Chen, J. M. Dawson, R. W. Huff, and T. Katsouleas, Phys. Rev. Lett. **54**, 693 (1985).

[3] J. B. Rosenzweig, B. Breizman, T. Katsouleas, and J. J. Su, Phys. Rev. A **44**, R6189 (1991).

[4] W. Lu, C. Huang, M. Zhou, W. B. Mori, and T. Katsouleas, Phys. Rev. Lett. **96**, 165002 (2006).

[5] I. Blumenfeld, C. E. Clayton, F.-J. Decker, M. J. Hogan, C. Huang, R. Ischebeck, R. Iverson, C. Joshi, T. Katsouleas, N. Kirby, W. Lu, K. A. Marsh, W. B. Mori, P. Muggli, E. Oz, R. H. Siemann, D. Walz, and M. Zhou, Nature **445**, 741 (2007).

[6] K. V. Lotov, Phys. Plasmas **14**, 023101 (2007).

[7] S. Lee, T. Katsouleas, R. G. Hemker, E. S. Dodd, and W. B. Mori, Phys. Rev. E **64**, 045501 (2001).

[8] J. Vieira and J. T. Mendonca, Phys. Rev. Lett. **112**, 215001 (2014).

[9] P. Mora and T. M. Antonsen, Phys. Plasmas **4**, 217 (1997).

[10] N. Jain, J. Palastro, T. M. A. Jr., W. B. Mori, and W. An, Phys. Plasmas **22**, 023103 (2015).

[11] M. J. Hogan, T. O. Raubenheimer, A. Seryi, P. Muggli, T. Katsouleas, C. Huang, W. Lu, W. An, K. A. Marsh, W. B. Mori, C. E. Clayton, and C. Joshi, New J. Phys. **12**, 055030

(2010).

[12] T. Katsouleas, S. Wilks, P. Chen, J. M. Dawson, and J. J. Su, Particle Accelerators **22**, 81 (1987).

[13] J. D. Jackson, *Classical Electrodynamics (Chapter 14)*, 3rd ed. (Wiley, New York, 1999).

[14] J. J. Su, T. Katsouleas, J. M. Dawson, P. Chen, M. Jones, and R. Keinigs, IEEE Trans. Plasma Sci. **15**, 192 (1987).